





JAAP PEDERSEN¹, KAI HOPPMANN-BAUM², JANINA
ZITTEL³, THORSTEN KOCH⁴

**Blending hydrogen into natural gas:
An assessment of the capacity of the
German gas grid
— Technical Report —**

¹  0000-0003-4047-0042

²  0000-0001-9184-8215

³  0000-0002-0731-0314

⁴  0000-0002-1967-0077

The content of this report is also available as publication in Operations Research Proceedings 2021. Please always cite as:
Pedersen, J., Hoppmann-Baum, K., Zittel, J., Koch, T. (2022). Blending Hydrogen into Natural Gas: An Assessment of the Capacity of the German Gas Grid. In:
Trautmann, N., Gnani, M. (eds) Operations Research Proceedings 2021. OR 2021. Lecture Notes in Operations Research. Springer, Cham. https://doi.org/10.1007/978-3-031-08623-6_28

Zuse Institute Berlin
Takustr. 7
14195 Berlin
Germany

Telephone: +49 30 84185-0
Telefax: +49 30 84185-125

E-mail: bibliothek@zib.de
URL: <http://www.zib.de>

ZIB-Report (Print) ISSN 1438-0064
ZIB-Report (Internet) ISSN 2192-7782

Blending hydrogen into natural gas: An assessment of the capacity of the German gas grid — Technical Report —

Jaap Pedersen¹[0000-0003-4047-0042], Kai Hoppmann-Baum^{1,2}[0000-0001-9184-8215],
Janina Zittel¹[0000-0002-0731-0314], and Thorsten Koch^{1,2}[0000-0002-1967-0077]

¹ Zuse Institute Berlin, Berlin, Germany
pedersen@zib.de

² Technical University Berlin, Berlin, Germany

Abstract. In the transition towards a pure hydrogen infrastructure, utilizing the existing natural gas infrastructure is a necessity. In this study, the maximal technically feasible injection of hydrogen into the existing German natural gas transmission network is analysed with respect to regulatory limits regarding the gas quality. We propose a transient tracking model based on the general pooling problem including linepack. The analysis is conducted using real-world hourly gas flow data on a network of about 10,000 km length.

1 Introduction

For a success of the *Energiewende*, it is necessary to mitigate volatile renewable energy sources, such as wind and solar power, and to prevent greenhouse gas emissions which are hard to reduce, e.g. from the industrial or heating sector. To tackle these challenges, green hydrogen as a flexible, regenerative, and storable energy carrier is going to play a key role in the future energy system.

With its National Hydrogen Strategy (NHS) [1], the German government defines a first general framework for a future hydrogen economy. As only a small share of the predicted demand is going to be covered by domestically produced green hydrogen, large amounts need to be imported and transported to the consumers. In the transition phase towards a pure hydrogen infrastructure, there is a growing interest in blending hydrogen into the existing natural gas grid, which ensures a guaranteed outlet and thereby incentivizes hydrogen production [2,3]. Despite the potential of blending hydrogen into gas grid, there are technical, economic, and regulatory challenges. No significantly increasing risk is given for blending hydrogen in low concentration. However, there are further regulatory limits regarding on the quality of provided natural gas [4,5].

To determine the maximal feasible injection of hydrogen into the existing natural gas grid, we propose a transient hydrogen propagation model, that takes different regulatory and technical limits into account. It is based on the general

pooling problem [6] extended by a linepack formulation. The assessment is performed a posteriori on measured hourly gas flow data of one of Europe's largest transmission network operators.

The mathematical formulation of the hydrogen propagation model and its notation is described in Section 2. An extension to a sequential hydrogen propagation model is given in Section 3. In Section 4, the considered network and data is presented. The results of the case study are discussed in Section 5. Finally, a short conclusion and outlook is given in Section 6.

2 Hydrogen propagation model

Let $G = (V, A)$ be a directed graph representing the gas network, where V denotes the set of nodes and A the set of arcs. The set of nodes V consists of entry nodes V^+ , exit nodes V^- , and inner nodes V^0 , i.e. $V = V^+ \dot{\cup} V^- \dot{\cup} V^0$. The set of arcs A consists of the set of pipelines $A^{\text{pi}} \subseteq A$ and the set of non-pipe elements $A^{\text{np}} := A \setminus A^{\text{pi}}$. Moreover, we further distinguish the set of compressing arcs, a subset of the non-pipe elements, i.e. $A^{\text{cs}} \subseteq A^{\text{np}}$.

For a discrete-time horizon $T := \{t_1, t_2, \dots, t_k\}$, where $\tau_t = t_t - t_{t-1}$ denotes the elapsed time between two subsequent time steps t and $t-1$, measured gas flow data is provided for each time step $t \in T$. In particular, each entry i in V^+ has a given inflow $s_{i,t} \in \mathbb{R}_{\geq 0}$, and each exit j in V^- has a given outflow $d_{j,t} \in \mathbb{R}_{\geq 0}$ for each time step $t \in T$. For each node $i \in V$ and time $t \in T$, measured values for the pressure $p_{i,t}$ and the temperature $T_{i,t}$ are given. For each pipeline $a = (l, r) \in A^{\text{pi}}$, the flow into a at l and out of a at r is given and denoted by $f_{a,t}^l, f_{a,t}^r \in \mathbb{R}$ at time $t \in T$, respectively. Note, that if $f_{a,t}^l < 0$ gas flows out of the pipe a at l and if $f_{a,t}^r < 0$ gas flows into the pipe a at r . The amount of gas stored in each pipeline $a \in A^{\text{pi}}$, also known as *linepack*, is denoted by $F_{a,t}$ for each time step $t \in T$. As the linepack is not available in the measured data, it is calculated using the *equation of state for real gases* and the existing quantities, see Section 2.2. For each non-pipe element $a \in A^{\text{np}}$, a single flow value $f_{a,t}$ is given at time $t \in T$. Let A_i^{ind} be the set of arcs $a \in A$ incident at node i . W.l.o.g, we assume that each entry $i \in V^+$ has exactly one adjacent arc with flow greater equal to zero.

Additionally, a subset of entry nodes $V_{H_2}^+ \subseteq V^+$ is selected where hydrogen injection is possible. The variable $\tilde{w}_{i,t} \in [0, q_{i,t}^{UB}]$ denotes the hydrogen mass fraction for each node $i \in V$ at time $t \in T$, where $q_{i,t}^{UB} \in [0, 1]$ represents its upper bound. Additionally, let $w_{a,t}, w_{a,t}^l, w_{a,t}^r \in [0, 1]$ denote the hydrogen mass fraction in the pipe, at l , and at r for each pipeline $a = (l, r) \in A^{\text{pi}}$ at time $t \in T$, respectively. Throughout this paper, the term *fraction* refers to the mass fraction. However, it is easily translated to the *volume fraction* (vol.-%), which is usually used to describe regulatory and technical limits, and vice versa. Finally, let $V_{a,t}$ denote the absolute amount of hydrogen in a pipeline $a \in A^{\text{pi}}$ at time $t \in T$.

2.1 Mixing in nodes

As gas flows from entries towards exits, it is mixed at nodes with at least two sources of inflow. We assume a linear blending behaviour, i.e. the hydrogen fraction at the mixing node is simply the amount of hydrogen flowing into the node divided by the total amount of gas entering it. The amount of hydrogen flowing into a node i is given by the product of the flow $f_{i,a,t}^{in}$ and its hydrogen fraction $w_{i,a,t}^{in}$ into node i over arc a at time step t . In particular, we formulate the mixing process as follows

$$\tilde{w}_{i,t} \sum_{a \in A_i^{ind}} f_{i,a,t}^{in} = \sum_{a \in A_i^{ind}} w_{i,a,t}^{in} f_{i,a,t}^{in} \quad \forall i \in V \setminus V^+, \forall t \in T \quad (1)$$

$$f_{i,a,t}^{in} = \begin{cases} f_{a,t}, & a = (j,i) \in A^{np} \wedge f_{a,t} > 0 \\ -f_{a,t}, & a = (i,j) \in A^{np} \wedge f_{a,t} < 0 \\ f_{a,t}^i, & a = (j,i) \in A^{pi} \wedge f_{a,t}^i > 0 \\ -f_{a,t}^i, & a = (i,j) \in A^{pi} \wedge f_{a,t}^i < 0 \\ 0, & \text{otherwise} \end{cases} \quad \forall a \in A_i^{ind} \quad (2)$$

$$w_{i,a,t}^{in} = \begin{cases} \tilde{w}_{j,t}, & a = (j,i) \in A^{np} \wedge f_{a,t} > 0 \\ \tilde{w}_{j,t}, & a = (i,j) \in A^{np} \wedge f_{a,t} < 0 \\ w_{a,t}^i, & a = (j,i) \in A^{pi} \wedge f_{a,t}^i > 0 \\ w_{a,t}^i, & a = (i,j) \in A^{pi} \wedge f_{a,t}^i < 0 \\ 0, & \text{otherwise} \end{cases} \quad \forall a \in A_i^{ind} \quad (3)$$

Note that non-pipe elements forward the hydrogen fraction at the outgoing node, e.g. $w_{i,a,t}^{in} = W_{j,t}$ if $f_a > 0$ for $a = (j,i) \in A^{np}$. Also note, that for each node $i \in V \setminus V^+$ with exactly one incoming arc (j,i) , the hydrogen fraction at the node is equal to the hydrogen fraction of the incoming flow and the hydrogen fraction has an arbitrary value for each node $i \in V \setminus V^+$ with zero inflow. Finally, we assume that the hydrogen fraction of the flow on all outgoing arcs is equal to the hydrogen fraction at the leaving node i . Figure 1 shows a mixing node with two incoming flows and one outgoing flow.

2.2 Mixing and linepack in pipelines

To keep track of the amount of hydrogen in the network over time, we need to consider the amount of gas stored in each pipeline $(l,r) \in A^{pi}$, i.e., the linepack. However, as the linepack is not directly measured, we determine the linepack of gas in a pipeline $a = (l,r) \in A^{pi}$ for a time $t \in T$ using the equation of state for real gases

$$p = R_s \rho T z_a \quad (4)$$

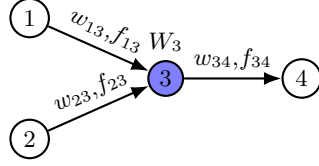


Fig. 1: Mixing at node with two incoming arcs

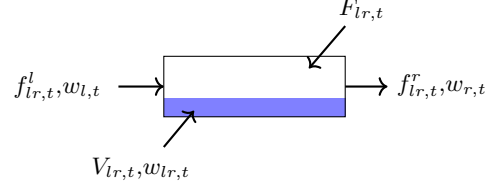


Fig. 2: Inflow and outflow of a pipeline with flow from left to right including linepack

where p , R_s , ρ , T , and z_a denote the pressure, the specific gas constant, the density, the temperature, and the compressibility factor of the gas, respectively. The pressure p and temperature T in a pipeline $a = (l, r)$ at time t is approximated by the arithmetic mean of the pressure and temperature at the end nodes l and r

$$p_{ave,t} = \frac{p_{l,t} + p_{r,t}}{2}, \quad T_{ave,t} = \frac{T_{l,t} + T_{r,t}}{2}, \quad \forall a = (l, r) \in A^{\text{pi}} \wedge t \in T.$$

We assume the values of R_s and z_a to be constant. With the definition of the density, i.e., mass per volume, the gas linepack $F_{a,t}$ of a pipeline a at time t is obtained by

$$F_{a,t} = \frac{p_{ave,t} v_a}{R_s T_{ave,t} z_a} \quad \forall a = (l, r) \in A^{\text{pi}} \wedge t \in T \quad (5)$$

where v_a denotes the volume of the pipeline a .

We assume instant mixing, i.e., the hydrogen fraction is always equal over the whole length of the pipeline and adapts immediately, the hydrogen fraction in the pipeline is described by

$$w_{a,t} F_{a,t} = w_{a,t-1} F_{a,t-1} + w_{a,t}^l f_{a,t}^l \tau_t - w_{a,t}^r f_{a,t}^r \tau_t \quad \forall a = (l, r) \in A^{\text{pi}}, \forall t \in T \quad (6)$$

$$w_{a,t}^r = \begin{cases} w_{a,t}, & f_{a,t}^r \geq 0 \\ \tilde{w}_{r,t}, & f_{a,t}^r < 0 \end{cases} \quad \forall a = (l, r) \in A^{\text{pi}}, \forall t \in T \quad (7)$$

$$w_{a,t}^l = \begin{cases} \tilde{w}_{l,t}, & f_{a,t}^l \geq 0 \\ w_{a,t}, & f_{a,t}^l < 0 \end{cases} \quad \forall a = (l, r) \in A^{\text{pi}}, \forall t \in T \quad (8)$$

where (6) describes the change of linepack over time and the mixing process in the pipeline, and (7)-(8) consider the flow direction w.r.t the hydrogen fraction at l and r of pipe $a = (l, r)$. An exemplary pipe is shown in Figure 2.

2.3 Objective and complete model

As our goal is to assess the hydrogen capacity of the gas network, the objective is to maximize the technically feasible hydrogen injection for the given set of

entry nodes $V_{H_2}^+ \subseteq V^+$ over the considered time horizon T . However, to obtain a smooth operation, we introduce a weight $\mu_{i,t}$ to penalize changes in hydrogen fraction at the entry nodes $V_{H_2}^+$ between time $t-1$ and t . The hydrogen propagation model is defined as the following linear programming formulation

$$\text{HPM: } \max_{W,w,V} \sum_{t \in T} \sum_{i \in V_{H_2}^+} \tilde{w}_{i,t} s_{i,t} - \mu_{i,t} |\Delta \tilde{w}_{i,t}| \quad (9)$$

$$\text{s.t. (1) - (8)}$$

$$0 \leq \tilde{w}_{i,t} \leq q_{i,t}^{UB} \quad \forall i \in V \setminus V^+, \forall t \in T \quad (10)$$

$$0 \leq \tilde{w}_{i,t} \leq 1 \quad \forall i \in V_{H_2}^+, \forall t \in T \quad (11)$$

$$\tilde{w}_{i,t} = 0 \quad \forall i \in V^+ \setminus V_{H_2}^+, \forall t \in T \quad (12)$$

where $|\Delta \tilde{w}_{i,t}| = |\tilde{w}_{i,t} - \tilde{w}_{i,t-1}|$ at an entry $i \in V_{H_2}^+$ at time t , which can easily be linearized.

3 Sequential hydrogen propagation model

Even though the hydrogen propagation model in Section 2 is a continuous LP, difficulties occur when the model is solved for large gas networks and long time periods. Thus, the time period and input data are split into smaller overlapping time horizons, which are solved iteratively. For each iteration, we define the starting state based on the previous solution.

However, hydrogen bounds may be violated, see (10), when considering multiple successive iterations as future flows are not available. Thus, to ensure feasibility across multiple iterations, slack variables for the hydrogen limits on critical elements, i.e., exits and compressor stations, are introduced. Let $\sigma_{i,t}^d \in \mathbb{R}_{\geq 0}$ be the slack variable on the hydrogen upper bound of exit $i \in V^-$ at time t . As the hydrogen bound of a compressor station $a = (i, j) \in A^{\text{cs}}$ is imposed on its outgoing node i , let $\sigma_{i,t}^a \in \mathbb{R}_{\geq 0}$ be the slack variable on the hydrogen upper bound of this node i at time t . To penalize the usage of slack variables, let $\kappa_{i,t}$ and $\gamma_{i,t}$ be penalty weights for using slack $\sigma_{i,t}^d$ on exit $i \in V^-$ and slack $\sigma_{i,t}^a$ on the outgoing node i of compressor $a = (i, j) \in A^{\text{cs}}$ at time t , respectively. Thus, **HPM** is extended to

$$\text{sHPM: } \max_{W,w,V,\sigma^d,\sigma^{\text{cs}}} \sum_{t \in T} \left(\sum_{i \in E} \tilde{w}_{i,t} s_{i,t} - \mu_{i,t} |\Delta \tilde{w}_{i,t}| - \sum_{i \in V^-} \kappa_{i,t} \sigma_{i,t}^d - \sum_{a=(i,j) \in A^{\text{cs}}} \gamma_{i,t} \sigma_{i,t}^a \right)$$

$$\text{s.t. (1) - (8), (11), (12)}$$

$$0 \leq \tilde{w}_{i,t} - \sigma_{i,t}^d \leq q_{i,t}^{UB} \quad \forall i \in V^-, \forall t \in T$$

$$0 \leq \tilde{w}_{i,t} - \sigma_{i,t}^{\text{cs}} \leq q_{i,t}^{UB} \quad \forall \text{cs} = (i, j) \in A^{\text{cs}}, \forall t \in T$$

$$\begin{aligned}\sigma_{i,t}^d &\in \mathbb{R}_{\geq 0} & \forall i \in V^-, \forall t \in T \\ \sigma_{i,t}^{cs} &\in \mathbb{R}_{\geq 0} & \forall cs = (i,j) \in A^{cs}, \forall t \in T.\end{aligned}$$

As it is more important to stay technically feasible at compressor stations than at exit nodes³, a *sequential hydrogen propagation algorithm* is formulated taking this hierarchy into account. If no feasible solution is found for **HPM**, in the next stage **sHPM** is solved where only exit slacks are allowed to be nonzero. If still no feasible solution is found, **sHPM** is solved again with both exit and compressor slacks in the final stage. Note, that the final stage of the **sHPM** is always feasible as all hydrogen bounds can be lifted by introducing enough slack. The complete sequential hydrogen propagation algorithm is stated in Algorithm 1.

Algorithm 1: Sequential hydrogen propagation algorithm

Input : Hydrogen propagation model formulation **HPM**, **sHPM**
Output: Feasible solution SOL

```

1 SOL ← solve HPM
2 if HPM is infeasible then
3   SOL ← solve sHPM with  $\sigma_{i,t}^{cs} = 0 \ \forall cs = (i,j) \in A^{cs} \wedge \forall t \in T$ 
4   if sHPM is infeasible then
5     SOL ← solve sHPM
6 return SOL
```

4 Case Study

Our analysis of the hydrogen capacity is conducted on a major part of the German gas grid using measured hourly gas flow data from the time period April to December 2020⁴. In the time period considered, there are frequent changes in the topology of the network, i.e. over 50 network configurations lasting from one hour up to 30 days. Hence, the sequential hydrogen propagation model from Section 3 is solved. A three-day rolling horizon with a two-day overlap is chosen to split the input data.

The network consists of 8600 nodes, with 56 entry and over 1000 exit nodes, and 10000 arcs. For hydrogen injection, 20 entries in Northwestern Germany are chosen in consultation with experts at the TSO, taking the general location of green hydrogen projects from the NEP Gas 2020-2030 [8] into account. The full network is shown in Fig. 3.

Besides technical restrictions regarding compressor stations, an important measure is the gas interchangeability represented by the Wobbe-Index *WI* at

³ Compressor parts do not work properly if the hydrogen fraction exceeds 10% [7]

⁴ missing period 09/17/2020-09/24/2020



Fig. 3: Complete network, volatile hydrogen entry nodes $V_{H_2}^+$, exit nodes V^-

exit nodes. Based on regulatory limits for WI and its behaviour for hydrogen/gas mixtures defined in [9,10], the permitted hydrogen fraction at exit nodes is determined a priori and ranges between 7 – 18 vol.-%.

In this study, an hydrogen limit of 10 vol.-% is imposed on compressor stations, cf. [7]. For all inner nodes not adjacent to an active compressor station, we set the hydrogen limit to 1.0. In the following, we consider three scenarios, which differ in the hydrogen limit on exit nodes. **H2-10**: At each exit $i \in V^-$ and time t , $q_{i,t}^{UB}$ is determined by the limits on WI and must not be greater than 10 vol.-%. **H2-WI**: At each exit $i \in V^-$ and time t , $q_{i,t}^{UB}$ is only based on WI . **H2-5**: The exit nodes are categorized in three groups, *country borders* with $q_{i,t}^{UB} = 10$ vol.-%, *industry-like exits* with $q_{i,t}^{UB} = 5$ vol.-%, and all other exits with limits based on the WI .

5 Results

The amount of hydrogen injected into the network is 11.2, 12.2, and 5.7 TWh for H2-10, H2-WI, and H2-5, respectively. As comparison, the amount of hydrogen given by a constant injection of 10 vol.-% at each entry $i \in V_{H_2}^+$ in each time step $t \in T$ without respecting any bounds results in 12 TWh and the planned capacity for green hydrogen in Germany is 14 TWh by 2030 according to [1].

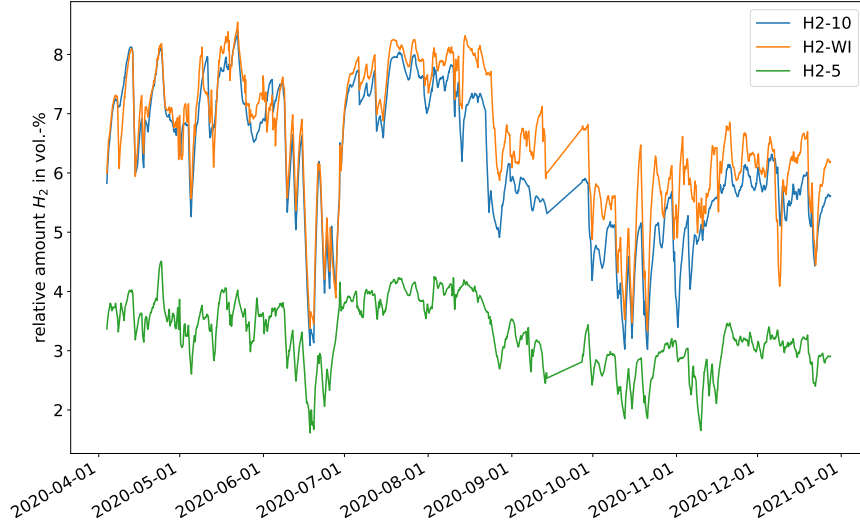


Fig. 4: Relative amount of hydrogen stored in the network for H2-10 (blue), H2-WI (orange), H2-5 (green) for the time period April to December 2020

The relative amount of hydrogen stored in the network at time t is shown in Fig. 4. H2-WI shows the highest amount of hydrogen in the network peaked in

May with over 8 vol.-%, followed by a slightly smaller amount in H2-10. Even though the limits for hydrogen at exits is more relaxed in H2-WI, the compressor restrictions are the same. Thus, only locally used, not recompressed gas may contain more than 10 vol.-% hydrogen, which usually refers to smaller entries. By imposing the much smaller bounds on *industry-like* exits in H2-5, the overall level of injection reduces by around 50% compared to the other two scenarios. In September approaching winter, the overall gas level increases with gas injection from Eastern non-hydrogen entries. Therefore, the hydrogen level drops in all scenarios.

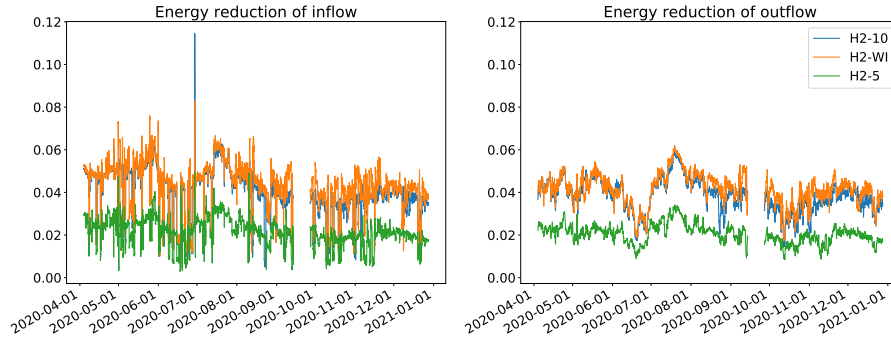


Fig. 5: Reduction in energy content of inflow (left) and outflow (right) for H2-10 (blue), H2-WI (orange), H2-5 (green) for the time period April to December 2020

By blending hydrogen into the gas grid, the energy content of the mixed gas is reduced due to the smaller energy density of hydrogen compared to natural gas if the same standard volume flow is assumed. Figure 5 shows the overall energy reduction of the inflow (left) and outflow (right) for the considered time period in all scenarios. Again, scenarios H2-10 and H2-WI do not differ much, see above. The energy reduction lies between 2 to 8% with singular peaks up to 12% (in scenario H2-WI) for the inflow and between 4 to 6% for the outflow. For scenario H2-5, the reduction of energy lies between 1 and 4% for both inflow and outflow.

Fig. 6 shows the count of the hydrogen fraction at hydrogen entries $V_{H_2}^+$ for active entries and time steps. An entry is active if the inflow is greater than 0. In H2-10 the H_2 entries can inject 10 vol.-% hydrogen most of the time. This is expected as this is the upper bound given for both exits and compressor stations. By removing the 10 vol.-% limit in H2-WI, the distribution is shifted to the right between 0.1 and 0.2. In H2-5, the distribution is centered at 5 vol.-% hydrogen representing the tightest bound given by *industry-like exits*. Whenever the first stage of the **sHPM**, i.e., **HPM** described in Section 2, is infeasible, slack has to be used, which forces hydrogen injection towards zero. This is represented in

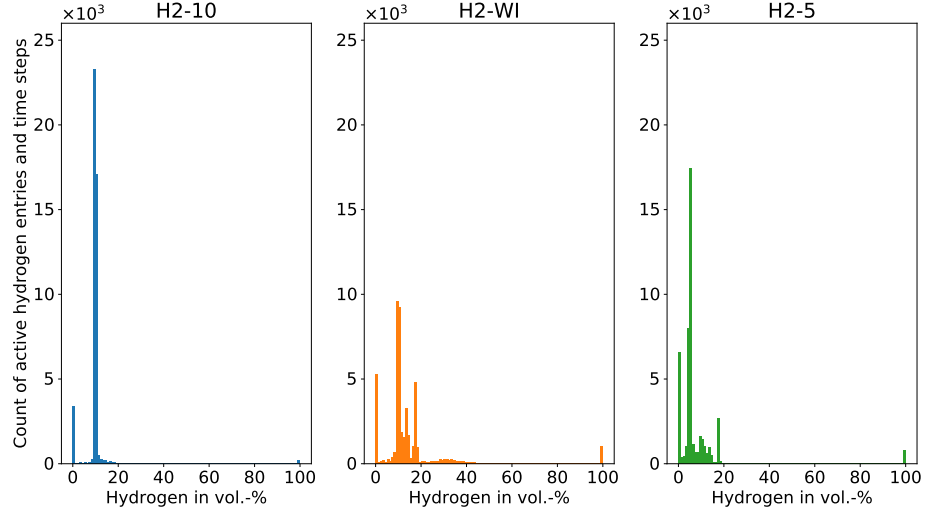


Fig. 6: Histogram of H_2 fraction at active hydrogen entries over the whole time period for all scenarios, H2-10 (left), H2-WI (middle), H2-5(right).

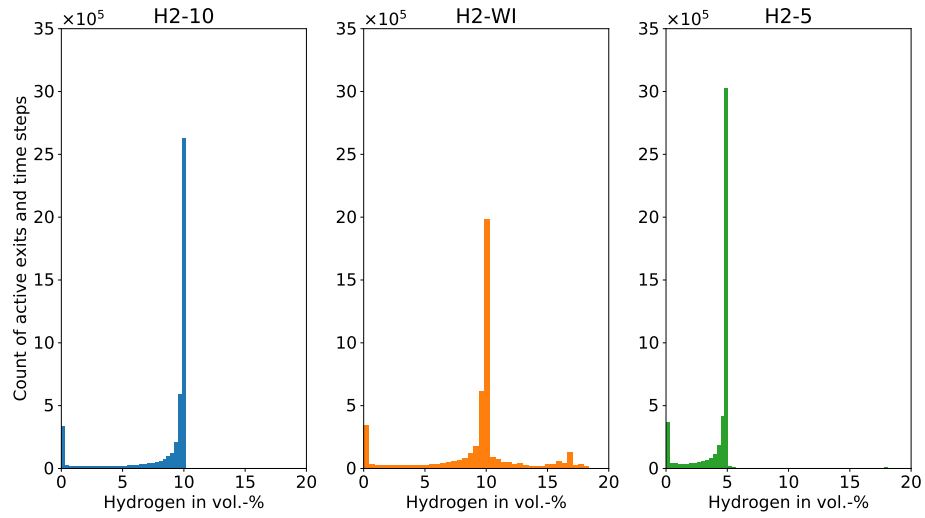


Fig. 7: Histogram of H_2 fraction at active exits (right) over the whole time period for all scenarios, H2-10 (left), H2-WI (middle), H2-5(right).

the peaks at 0% hydrogen. The upper bounds on the exits in the three scenarios can be recognized in the histogram of active exits, shown in Fig. 7. Again, the active exits are counted for each time step where exits are active if the outflow is greater than 0.

Fig. 8 shows the **gas inflow** and the **hydrogen fraction** of an exemplary entry with a high volatility in the hydrogen fraction in H2-WI and H2-5. The gas inflow for all scenarios is the same. A threshold of 3% of maximal gas inflow is set to neglect gas inflow and hydrogen fraction. In H2-10, the hydrogen bounds are dominated by both the compressor stations as well as the exits leading to an almost constant hydrogen fraction of 10 vol.-% at this entry node. This behaviour can be observed at the other entries as well.

The hydrogen fraction becomes more volatile in H2-WI and even more so in H2-5. Towards the end of the time period, hydrogen fractions of up to 15 vol.-% are possible. However, the gas inflow significantly drops simultaneously. The gas is either used locally, i.e., without passing a compressor station, or is mixed with gas from different parts of the network allowing higher share of hydrogen.

Between May and August, the hydrogen fraction fluctuate around 5 vol.-% in H2-5 meaning this entry node supplies at least one industry-like exit node. The use of slack options forces the hydrogen input towards zero for short periods explaining the drops towards zero in the hydrogen fraction.

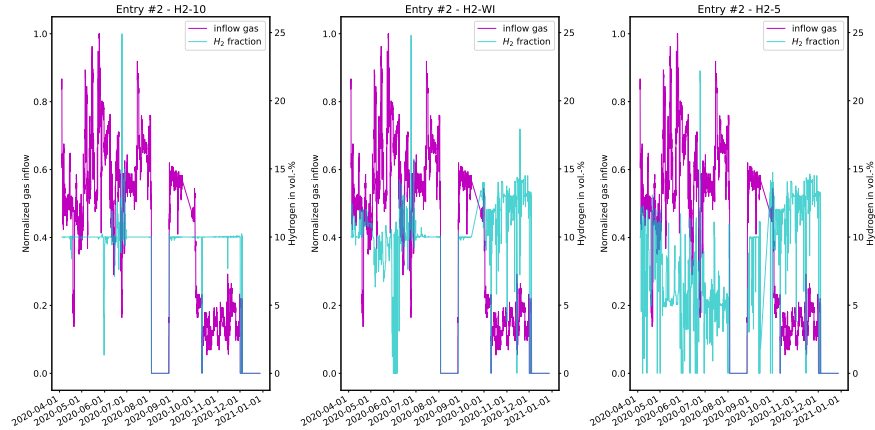


Fig. 8: **Gas inflow** and **hydrogen volume fraction** for a given entry for all scenarios, H2-10 (left), H2-WI (middle), H2-5(right)

6 Conclusion

With the proposed hydrogen propagation model, the hydrogen capacity of an existing gas network can be assessed. The analysis is performed on historically

gas flow data using a number of hydrogen injection location and imposing different bounds on exits and compressor stations. The first impression is that there is enough capacity to blend hydrogen into the gas grid in the transition phase.

However, by blending hydrogen into the grid, the gas quality and the energy content are reduced. The question remains if the security of supply is still given as greater flows or higher pressure gradients are needed to supply the nominated demand. Also, as hydrogen is referred to as “*energy transition’s champagne*”⁵ and only CO₂-neutral hydrogen should be used, one could include the segregation of hydrogen from the gas grid into the model.⁶

The considered time period is going to be extended to a full year to cover the complete seasonal cycle. In the future, we plan to integrate hydrogen tracking into the operation.

7 Acknowledgement

The work for this article has been conducted in the Research Campus MODAL funded by the German Federal Ministry of Education and Research (BMBF) (fund numbers 05M14ZAM, 05M20ZBM).

References

1. Federal Ministry for Economic Affairs and Energy: The National Hydrogen Strategy. 2020. <https://www.bmwi.de/Redaktion/EN/Publikationen/Energie/the-national-hydrogen-strategy.pdf>
2. Quarton, C. J., Samsatli, S.: Should we inject hydrogen into gas grids? Practicalities and whole-system value chain optimisation. *Applied Energy*, vol. 275, pp. 115-172, 2020, <https://doi.org/10.1016/j.apenergy.2020.115172>.
3. Quarton, C. J., Samsatli, S.: Power-to-gas for injection into the gas grid: What can we learn from real-life project, economic assessments and systems modelling? *Renewable and Sustainable Energy Reviews*, vol. 98, pp. 302-316, 2018, <https://doi.org/10.1016/j.rser.2018.09.007>
4. Melaina, M. W., Antonia, O., Penev, M.: Blending Hydrogen into Natural Gas Pipeline Networks: A Review of Key Issues. Technical Report, National Renewable Energy Laboratory, 2013, <https://www.nrel.gov/docs/fy13osti/51995.pdf>
5. Haeseldonckx, D., D’haeseleer, W.: The use of the natural-gas pipeline infrastructure for hydrogen transport in a changing market structure, *International Journal of Hydrogen Energy*, vol 32, pp. 1381-1386, 2007, <https://doi.org/10.1016/j.ijhydene.2006.10.018>
6. Haverly, C. A., *Studies of the behavior of recursion for the pooling problem*, ACM SIGMAP Bulletin, 25, 1978, <https://doi.org/10.1145/1111237.1111238>
7. Siemens Energy, Cascade Gastransport GmbH, Nowega GmbH. Whitepaper Wasserstoffinfrastruktur - tragende Säule der Energiewende. 2020 <https://www.get-h2.de/wp-content/uploads/200915-whitepaper-h2-infrastruktur-DE.pdf>

⁵ Claudia Kemfert in <https://www.tagesschau.de/wirtschaft/wasserstoff-technologie-101.html>

⁶ <https://www.fraunhofer.de/content/dam/zv/en/press-media/2021/april-2021/ikts-green-hydrogen-transportation-in-the-natural-gas-grid.pdf>

8. FNB-Gas. Netzentwicklungsplan Gas 2020-2030. 2021. <https://www.fnb-gas.de/netzentwicklungsplan/netzentwicklungsplaene/netzentwicklungsplan-2020/>
9. DVGW-Arbeitsblatt G 260: Gasbeschaffenheit. Bonn. März 2013
10. DVGW-Arbeitsblatt G 262: Nutzung von Gasen aus regenerativen Quellen in der öffentlichen Gasversorgung. September 2011